Received: 2 July 2019 | Revised: 28 October 2019 | Accepted: 3 December 2019

DOI: 10.1111/exd.14069

ORIGINAL ARTICLE

Experimental Dermatology WILEY

High bacterial colonization and lipase activity in microcomedones

Gwendal Josse[1] | Céline Mias[1] | Jimmy Le Digabel[1] | Jérôme Filiol[1] | Célia Ipinazar[1] | Aurélie Villaret[1] | Caroline Gomiero[1] | Marc Bevilacqua[2] | Daniel Redoules[1] | Thérèse Nocera[1] | Jean-Hilaire Saurat[3] | Etienne Gontier[2]

[1]Pierre Fabre Laboratories, Skin Research Center, Toulouse, France

[2]Bordeaux Imaging Center, Bordeaux, France

[3]Department of Clinical Pharmacology and Toxicology, University of Geneva, Geneva, Switzerland

Correspondence
Gwendal Josse, Pierre Fabre Laboratories, 2, rue Viguerie, BP3071, 31025 Toulouse Cedex 3, France.
Email: gwendal.josse@pierre-fabre.com

Abstract

Background: Although acne vulgaris has a multifactorial aetiology, comedogenesis and bacteria colonization of the pilosebaceous unit are known to play a major role in the onset of inflammatory acne lesions. However, many aspects remain poorly understood such as where and when is the early stage of the *Propionibacterium acnes* colonization in follicular unit? Our research aimed at providing a precise analysis of microcomedone's structure to better understand the interplay between *Propionibacterium acnes* and follicular units, and therefore, the role of its interplay in the formation of acne lesions.

Methods: Microcomedones were sampled using cyanoacrylate skin surface stripping (CSSS). Their morphology was investigated with multiphoton imaging and their ultrastructure with scanning electron microscopy (SEM) and transmission electron microscopy (TEM). Bacterial lipase activity in the microcomedones was quantified using a dedicated enzymatic test as well as a Fourier Transform Infra-Red (FTIR) analysis. The porphyrin produced by bacteria was analysed with HPTLC and fluorescence spectroscopy.

Results: The imaging analysis showed that microcomedones' structure resembles a pouch, whose interior is mostly composed of lipids with clusters of bacteria and whose outer shell is made up of corneocyte layers. The extensive bacteria colonization is clearly visible using TEM. Even after sampling, clear lipase activity was still seen in the microcomedone. A high correlation, $r = .85$, was observed between porphyrin content measured with HPTLC and with fluorescence spectroscopy. These observations show that microcomedones, which are generally barely visible clinically, already contain a bacterial colonization.

KEYWORDS

Acne vulgaris, electron microscopy, fluorescence, fourier transform infrared, hair follicle, Inflammation, multiphoton microscopy, *Propionibacterium acnes*

1 | INTRODUCTION

Acne vulgaris is a very common skin disease, typical of adolescents and young adults, with multifactorial aetiology, including comedogenesis, seborrhoea, bacteria colonization and inflammation.[1–3] The precise mechanism behind the onset of acne lesions is still not fully understood, and the role of *Propionibacterium acnes* is still largely discussed.[4,5] Although *P acnes* is observed in normal and acne skin, intense *P acnes* colonization of the sebaceous gland likely play a role in acne inflammation through bacterial antigens and creation of a biofilm.[4–6] The intense *C acnes* colonization causes inflammatory reactions and immune cell recruitment.[6] The bacteria's metabolism is also known to modify the skin's lipid composition. Namely, bacterial lipase activity liberates free fatty acids (FFA) from triglycerides (TG). Free fatty acids being much more viscous than TG, they contribute to the obstruction of the pilosebaceous unit, which then becomes anaerobic, leading to a *P acnes* proliferation. Direct *P acnes* signalling towards sebocytes also increases lipogenesis and contributes to inflammation.[7,8]

The obstruction of the pilosebaceous unit was described in 1971 by Plewig et al.[9] They introduced the concept of comedogenesis and demonstrated that comedones formation is due to an accumulation of corneocytes and hyperproliferation of ductal keratinocytes in the pilosebaceous unit.[9] Since then, it has been established microcomedones already present hyperproliferative features.[10] They are generally barely visible clinically, however, they can be seen at the histological level. Traditionally, microcomedone density has been determined using bright field optical microscopy of cyanoacrylate skin surface stripping (CSSS).[11] In this context, the ability to reduce the number of microcomedones over time is a classical criterion by which new anti-acne treatments are judged to be efficient.[11,12] Indeed, a large number of molecules have been developed to prevent comedogenicity.[13,14]

In vivo fluorescence imaging has also been widely employed for acne skin visualization because *P acnes* produces porphyrins, a family of pro-inflammatory metabolites[15,16] which exhibits a strong fluorescence under A-light ultraviolet (UVA) excitation.[17–19] Recently Xu et al confirmed through a systematic analysis that the skin red autofluorescence comes from *P acnes* porphyrin and that pure sebum present any red autofluorescence.[20] Also, Johnson et al showed that *P acnes* strains from acne skin produce more porphyrins than *P acnes* strain from normal skin do.[21] The in vivo imaging devices have not always been optimized for selecting the fluorescent wavelengths of interest. Patwardhan et al pointed out that the porphyrin most produced by *P acnes*, Coproporphyrin III, presents a fluorescence emission between 570 and 630 nm.[15]

However, many questions remain open, especially is *P acnes* colonization in the pilosebaceous unit starting as soon as microcomedone stage? And is it associated with a clear bacterial metabolism?

In order to address these questions, we firstly studied microcomedones' ultrastructure, secondly analysed their autofluorescence properties, and finally, we quantified the lipase activity.

2 | MATERIALS AND METHODS

2.1 | Cyanoacrylate skin surface stripping (CSSS)

Cyanoacrylate skin surface stripping is a rapid, simple and non-invasive method, removing only the superficial skin layer, the stratum corneum, using the robust glue cyanoacrylate. This method is employed to study corneocytes, follicular casts, microcomedones and a vast variety of microorganisms such as demodex. In this study, we used a commercial kit (S-Biokit, C/K Electronic). Briefly, two drops of cyanoacrylate were deposited on a polyethylene slide (thick: 175 µm, size: 1.5 × 6 cm). The slide was placed on the subjects' foreheads. After polymerization, occurring in 90 seconds, the slide was gently and tangentially removed from the skin surface and stored at 4°C until analysis. The CSSS samples were taken on prone acne subjects at the Hotel Dieu skin clinical centre Toulouse France, which is legally approved by of the French Health Ministry. All subjects gave their written consent and were examined by a physician.

Cyanoacrylate skin surface stripping sample imaging in dark field and epifluorescence microscopy. Cyanoacrylate skin surface stripping samples were directly imaged with dark field illumination using an Olympus BX43 microscope. All images were acquired on a 4× objective (NA 0.13). The mosaic imaging process performed the entire image using CellSens software (Olympus). Mosaic imaging in epifluorescence was performed with the same procedure, using a mCherry filter cube (Emission Wavelength: 605-665 nm; Excitation Wavelength: 540-580 nm) and a 120 W mercury vapour short arc lamp.

Quantification of microcomedone density from epifluorescence images. Microcomedone density and surface were assessed on the reconstituted images realized in autofluorescence mode using 4× objective. We developed a dedicated software to automatically detect the microcomedones on the fluorescence image and calculate the density (number/μm^2) and the surface (μm^2) of microcomedones for each CSS sample. The automatic detection is checked afterwards and manually corrected when necessary. The software analysis was validated through a comparison with a manual counting on 109 samples (linear correlation coefficient r = .88).

2.2 | CSSS sample structure imaging by multiphoton (MP) microscopy

Image acquisition was performed directly on CSSS samples on a Nikon A1MP microscope with a Spectra Physics MaiTai laser. The lens used for the acquisitions is a 25× with a numerical aperture of 1.1 The excitation wavelength was fixed to 820 nm. The autofluorescence was captured with three GaAsp non-descanned detectors corresponding to three spectral windows (blue: $\lambda < 492$ nm; green: $500 < \lambda < 550$ nm; red: $603 < \lambda < 656$ nm). The MP imaging was performed on samples from six subjects.

A complementary measurement was performed with a spectral detector. The 3D image was then divided into several zones according to different fluorescence signals.

2.3 | Microcomedone ultrastructure imaging by electronic microscopy

Microcomedones were isolated from CSSS samples and directly fixed with 2% (v/v) paraformaldehyde and 2.5% (v/v) glutaraldehyde in 0.1 mol/L sodium cacodylate buffer (pH 7.4) at 4°C overnight.

For TEM imaging, samples were washed in 0.1 mol/L sodium cacodylate buffer (pH 7.4) and then post-fixed in a mix 1% osmium tetroxide (v/v)/ 1% potassium ferricyanide K3Fe (CN)6 (wt/v) in same 0.1 mol/L sodium cacodylate buffer during 1 hour 30 at room temperature (RT) in the dark to enhance contrast.

After extensive washing in 0.1 mol/L sodium cacodylate buffer, samples were dehydrated through a series of graded ethanol, then infiltrated in series of mixtures of ethanol and epoxy resin (Epon 812; Delta Microscopies)—Graduated mixtures—followed by embedding in 100% resin overnight at RT. Next day, a new embedding in pure resin was made all day at RT before polymerization over a period between 24 and 48 hours at 60°C. Samples were then sectioned on an ultramicrotome (EM UC7; Leica Microsystems). Ultrathin sections (65 nm) were picked up on copper grids and were examined with a Transmission Electron Microscope (H7650; Hitachi) at 80 kV. For SEM, the fixed samples were imaged in scanning electron microscope (FEI Quanta200). Specimens were imaged under low vacuum (50 Pa) at different high voltage. Images were collected using the secondary electron detector. The analysis was performed on samples from six subjects.

2.4 | Fluorescence measurements

Fluorescence measurements were realized with Varioskan (Varioskan: 3001-78. Software SkanIt; Thermo Fisher Scientific). Wavelength of excitement was fixed at λ = 400 nm. Spectrum of emission was measured in range λ (400-800 nm). Comedones were transferred in an Eppendorf tube (Eppendorf). They were solubilized in a mix of solvents CHCl3/MeOH 150/150 µL homogenized with a vortexer and an ultrasonic bath during 15 minutes. Then samples were transferred to a quartz plate for the fluorescence measurements. After the analysis, microcomedone samples were transferred in Eppendorf tubes. Sample was then evaporated under Speed-Vac SPD 111V (Thermo Fisher Scientific) and under nitrogen before extraction for HPLC analysis. The analysis was performed on samples from 30 subjects.

2.5 | Quantitative porphyrin analysis by HPLC

The comedones samples after evaporation were suspended in 200 µL ethyl acetate and homogenized with a vortexer and an ultrasonic bath 25 kHz from Elma. After centrifugation, 2 × 20 µL of supernatant was pipetted for the analysis of lipids by HPTLC (high-performance thin-layer chromatography). Samples were concentrated by evaporation with Speed-Vac SPD 111V (Thermo Fisher Scientific). At this stage, samples can be kept in the dark at 4°C if needed and then reprocessed for HPLC (high-performance liquid chromatography).

45 µL acetic ccid, 5 µL formic acid, 50 µL hydrochloric acid (HCl) 6 mol/L and 100 µL of water were added for hydrolysis and solubilization. 200 µL ethyl acetate was added for partition of solvents. Finally, the suspension was mixed for 30 seconds in a vortexer and then centrifuged for 10 minutes at 14 000 trmin^{-1}. Three parts were analysed for each sample: (a) The lower phase (190 µL of HCl phase), which contains the porphyrins, was transferred via a pipette to another Eppendorf tube. (b) The supernatant (ethyl acetate phase) was transferred, evaporated and dissolved with 185 µL HCL 0.06 mol/L and 5 µL Formic Acid. (c) Pellet at the bottom of the tube was evaporated and dissolved with 2 µL HCl 6 mol/L, 183 µL HCl 0.06 mol/L and 5 µL formic acid. Prior to HPLC analysis, the extracts were mixed with 10 µL of mesoporphyrin IX at 10 µg mL^{-1} as an internal standard (Frontier Scientific).

Porphyrins were analysed using a HPLC chromatograph (Agilent HP 1100 Series) with a multiple wavelength detector (Agilent HP 1200 Series DAD SL) which offers multiple wavelength. The automatic sampler of the HPLC was programmed at a temperature of 4°C. The column used was a reversed-phase C18 HPLC column (Hypersil ODS (C18); 200 × 4.6 mm; 5 µm) attached to a pre-column or guard cartridge (Hypersil ODS 10 × 4 mm), with a flow of 1 mL min^{-1} and a 10 µL sample injection size. Oven of the column was heated at 30°C. Standard solutions of porphyrins were prepared in HCl in concentrations from 10 to 0.01 µg mL^{-1}. For the porphyrin analysis, 10 µL of sample was injected into the chromatograph at a flow rate of 1 mL min^{-1} with a total analysis time of 35 minutes. Phase A was prepared using 0.2 mol/L ammonium acetate buffer pH 5.1. Phase B was prepared from 90% HPLC methanol (Carlo Erba) and 10% acetonitrile (Merck or Carlo Erba). Elution was performed using a gradient programme starting with 70% phase A and 30% phase B with a final at 25 minutes with 10% phase A and 90% phase B. Then, 10 minutes of reconditioning with starting conditions. The analysis was performed on samples from 30 subjects.

2.6 | Chemicals and reagents for the HPLC analysis

Analyses were performed using solvents of analytical grade: methanol (MeOH) RS HPLC Gold and Acetonitrile for HPLC gradient, ethyl acetate ACS for analysis and chloroform (CHCl3) RPE for analysis were purchased from Carlo Erba. Hydrochloric acid (HCl) 1 N and formic acid 98%-100% for analyses were acquired from Merck (France or Darmstadt). Hydrochloric acid (HCl) 6 N and ammonium acetate for HPLC ≥ 99.0% were purchased from Sigma Aldrich. Acetic acid HiPerSolv Chromanorm for HPLC was acquired from VWR BDH Prolabo. Ultrapure water was obtained by Milli-Q system

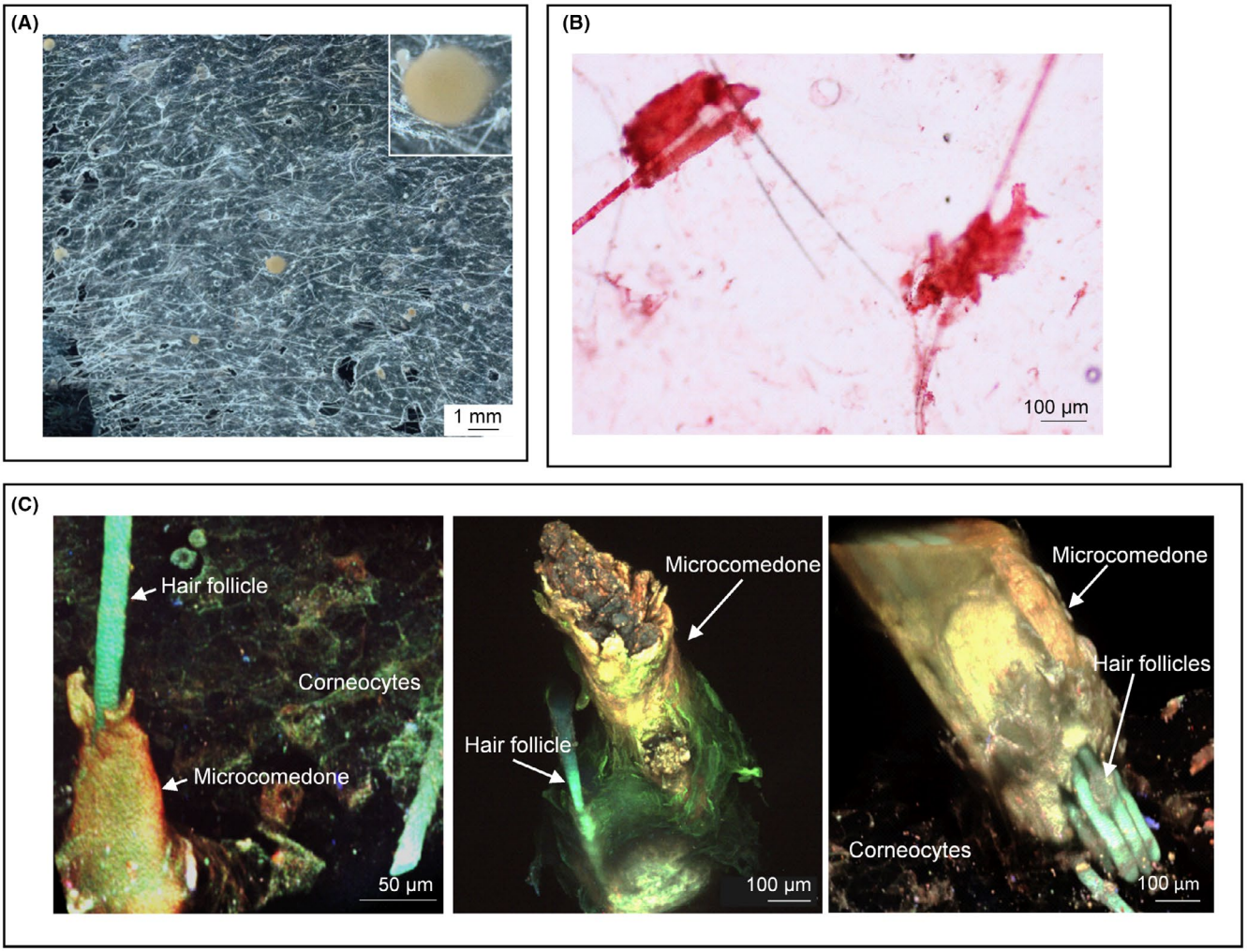

FIGURE 1 Structural analysis of microcomedones from cyanoacrylate skin surface stripping sample. A, Representative microscopic images of cyanoacrylate skin surface stripping sample (CSSS) samples using dark field mode, showing the presence of microcomedones, corneocytes network and hair follicles on skin surface layer. B, Representative images of lipid accumulation around and inside microcomedones on CSSS sample using O Red Oil staining in bright field microscopy. C, High-resolution 3D images of microcomedones observed on CSSS samples by multiphoton microscopy using autofluorescence mode

from Millipore. Standards of coproporphyrin I HCl, coproporphyrin III HCl, protoporphyrine IX, mesoporphyrin IX were purchased from Frontier Scientific.

2.7 | Lipase assay

Lipase activity was evaluated directly on cyanoacrylate samples using the EnzChek® lipase substrate (Thermo Fisher). Rapidly, in the presence of lipases, this substrate produces a green fluorescence. A reaction buffer was made containing 50 mmol/L Tris, 2 mmol/L $CaCl_2$, 0.1 mg/mL SB3-14 (3-[N,N-Dimethylmyristylammonio] propanesulfonate) and adjusted to pH 8.0 with HCl. The EnzChek lipase substrate was diluted to 50 µmol/L in the reactive buffer. The reaction buffer (50 µL) and substrate (50 µL) were mixed and equilibrated for 1 hour at RT before the addition of cyanoacrylate samples (5 punches of 4 mm/ sample) or lipase of porcine pancreas (as positive control, 1 µg/mL). After incubation, fluorescence was read on a Clariostar® microplate spectrofluorometer (BMG Labtech). Excitation and emission wavelengths were adjusted to 482 and 515 nm, respectively. The analysis was performed on samples from 17 subjects.

2.8 | Quantification of free fatty acid/triglyceride ratio by infrared spectroscopy

Microcomedones were isolated from the CSS samples and then solubilized in Chloroform/MeOH mix (1:1 vol:vol). ATR-FTIR spectra of the solubilized microcomedones were acquired in the 4000-670 cm^{-1} range on a Perkin Frontier spectrometer (Spectrum 400 FT-IR, Perkin Elmer). The ratio of the pick areas of free fatty acids (1710 cm^{-1}) and triglycerides (1740 cm^{-1}) was calculated. The analysis was performed on samples from 28 subjects.

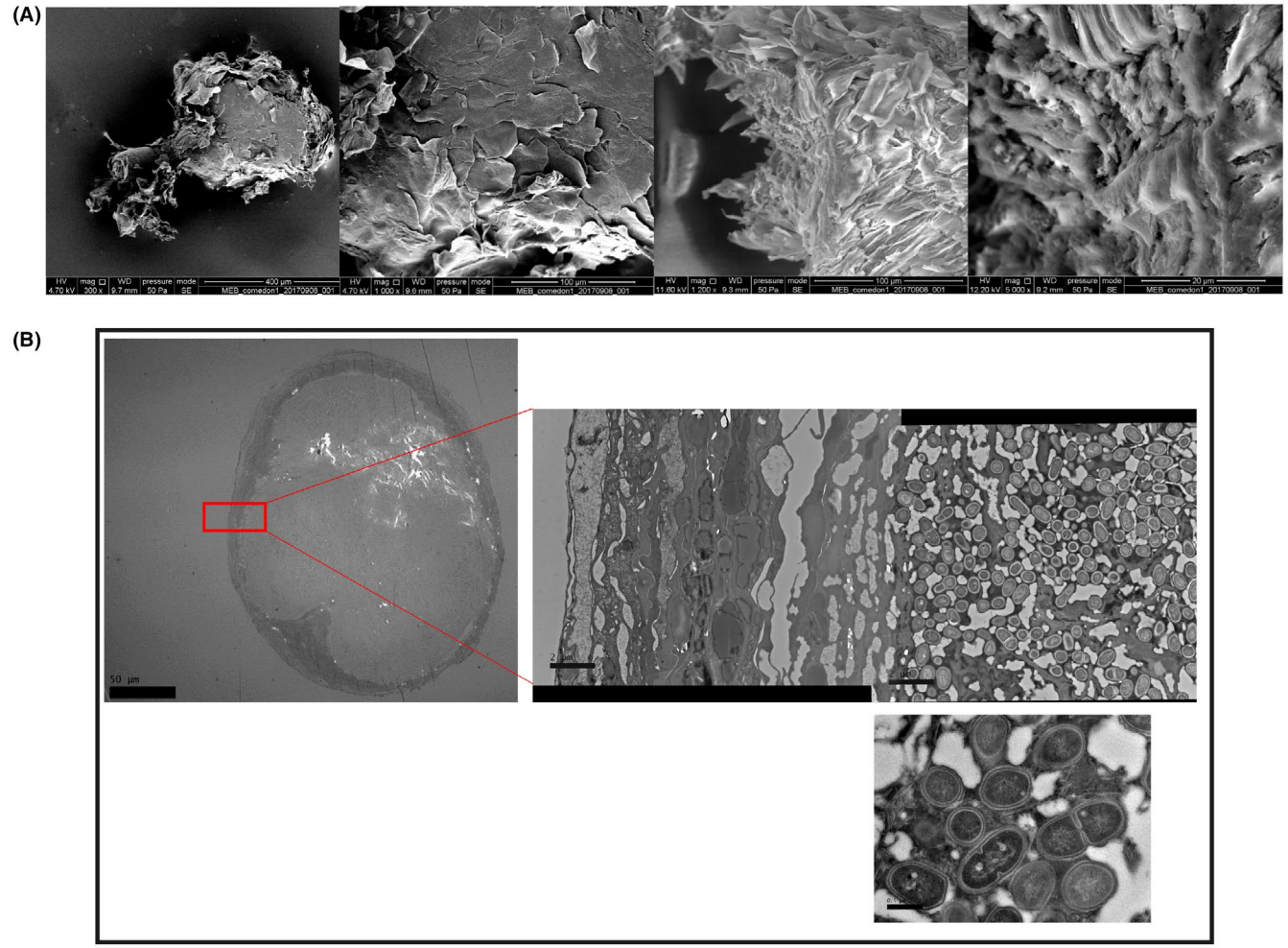

FIGURE 2 Ultrastructural analysis of microcomedones by electron microscopy. A, Representative images of microcomedones analysed by scanning electron microscopy, showing the overall view of a microcomedone. B, Representative images of microcomedones analysed by transmission electron microscopy, showing the overall pouch shape of microcomedone: corneocyte layers at exterior, cluster of *Propionibacterium acnes* bacteria inside the microcomedone and presence of lipids around the bacteria

2.9 | Lipid staining

Lipid content in the microcomedones was visualized directly on the CSSS samples using O Red Oil lipid-specific staining. CSSS samples were cut into 1 cm^2 pieces and directly transferred into propylene glycol 100% for 2 minutes at RT. Then, CSSS pieces were incubated in O Red Oil solution (Sigma Aldrich) for 10 minutes at RT. After sample washing in PBS1X, microscopic analysis using bright field mode was performed.

3 | RESULTS

3.1 | Structural analysis of microcomedones from cyanoacrylate skin surface stripping (CSSS) samples

Cyanoacrylate skin surface stripping was used to collect and study microcomedones and their associated bacterial activity at the superficial layer of the skin, the stratum corneum. Classically, CSSS samples have been visualized under a standard microscope using bright field mode. Here, we show that other microscopy modes are better suited for the analysis of microcomedones. Indeed, dark field mode gives a much better visualization of the different structures than bright field mode Figure 1A. Microcomedones, were easily distinguished, appearing as a rounded yellowy structure. Furthermore, lipid accumulation around and inside microcomedones was directly visualized on CSSS samples using O Red Oil staining, as shown in Figure 1B.

Using autofluorescence mode, multiphoton microscopy shows that it is possible to obtain high-resolution images of skin components without any preliminary labelling. As illustrated in Figure 1C, label-free 3D images of human CSSS samples revealed the structures of corneocytes, hair follicles and microcomedones with high quality. Indeed, CSSS totally maintained the integrity of superficial skin structures. As expected, we observed corneocyte paving forming a cohesive honeycomb pattern, and hair follicles appeared as well to be inserted individually or organized in bundles. We also observed the 3-D microcomedone structure appearing as a lipid-rich material covering the base of the hair follicle.

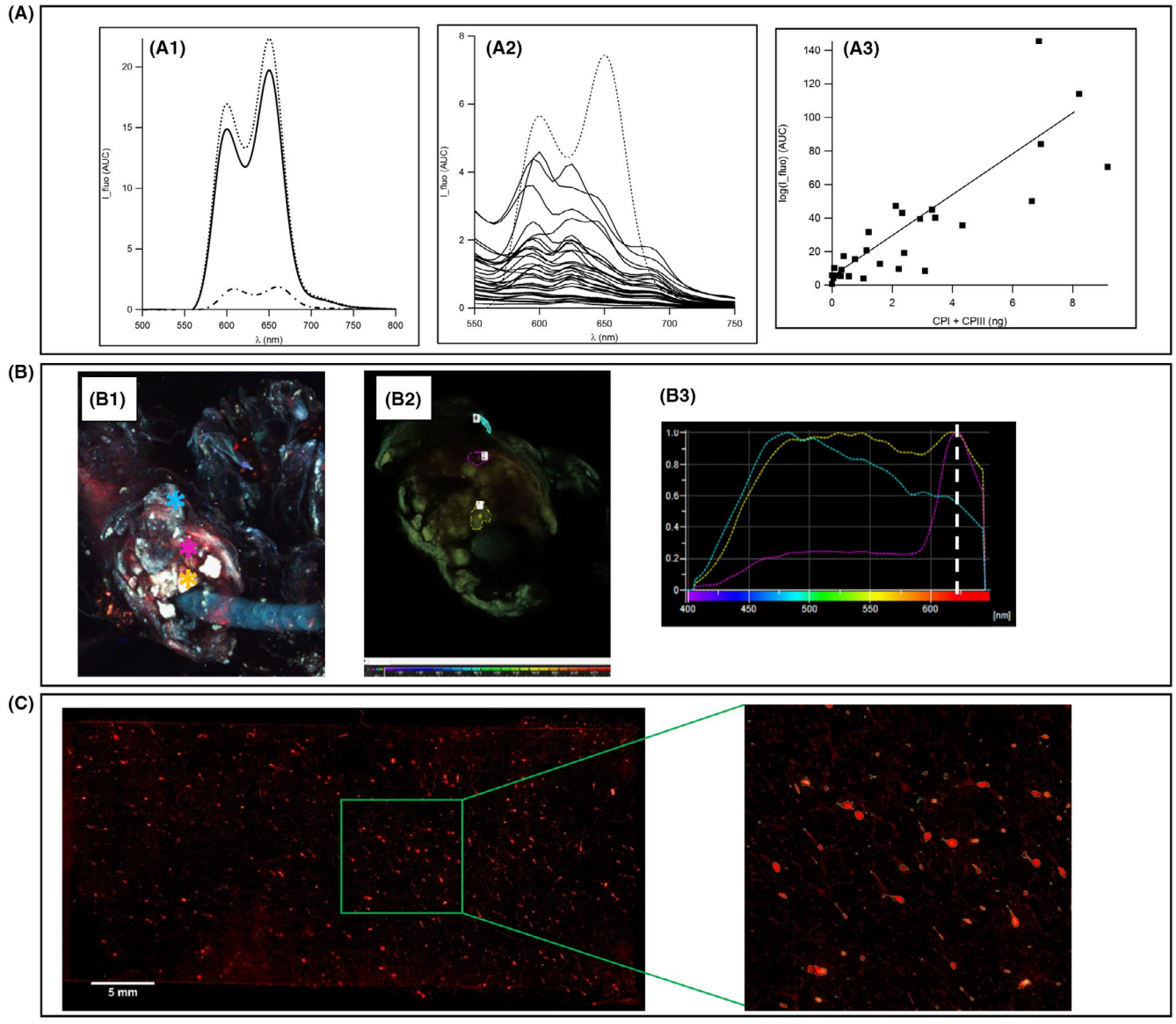

FIGURE 3 Determination of autofluorescence properties of porphyrins and quantification of microcomedone density on cyanoacrylate skin surface stripping samples. A, A1, Autofluorescence of porphyrins standards (dotted line: CPI; full line: CPIII; mixed line: PpIX). A2, Autofluorescence of solubilized microcomedones. In small red autofluorescence quantification (AUC between 560 and 665 nm) for all samples. A3, Correlation between red autofluorescence intensity (AUC between 560 and 665 nm) and the porphyrin amount from solubilized microcomedones determined by HPTLC analysis. B, B1-B2 Multiphoton images with NDD detectors (B1) and with spectral detector (B2) of label-free microcomedones on CSSS samples using autofluorescence mode. B3, Autofluorescence profiles of microcomedone computed from three different parts indicated in the image B2. C, Representative image of CSSS samples in epifluorescence microscopy using red autofluorescence mode. Microcomedone contour and density were automatically detected by an homemade software

The scanning electron microscopy revealed that the structure of microcomedones is surrounded with lot of layers of stratum corneum Figure 2A. Transmission electron microscopy of isolated microcomedones revealed their major components: the corneocyte layer, multilamellar lipid sheets and bacteria colonization. Inside microcomedones, many clusters of bacteria were localized. Moreover, bacteria were often observed being in division phase, this directly proves that they largely proliferate in the microcomedone Figure 2B. Thus, due to the great conservation of the structure integrity, CSSS is an effective method for studying microcomedone ultrastructure using electronic microscopy.

3.2 | Intrinsic porphyrin fluorescence in microcomedones

In order to check the presence of the porphyrins in the sampled microcomedones, two analyses were performed. Firstly, several large microcomedones were manually detached from the slide and solubilized with methanol/chloroform (1/1 vol/vol). Their fluorescence was then analysed with a highly sensitive fluorescence reader. Fluorescence spectra of solubilized microcomedones were detected in the 560-665 nm spectral region with two specific peaks: at 595 nm and 620 nm Figure 3A2), as for porphyrin standards

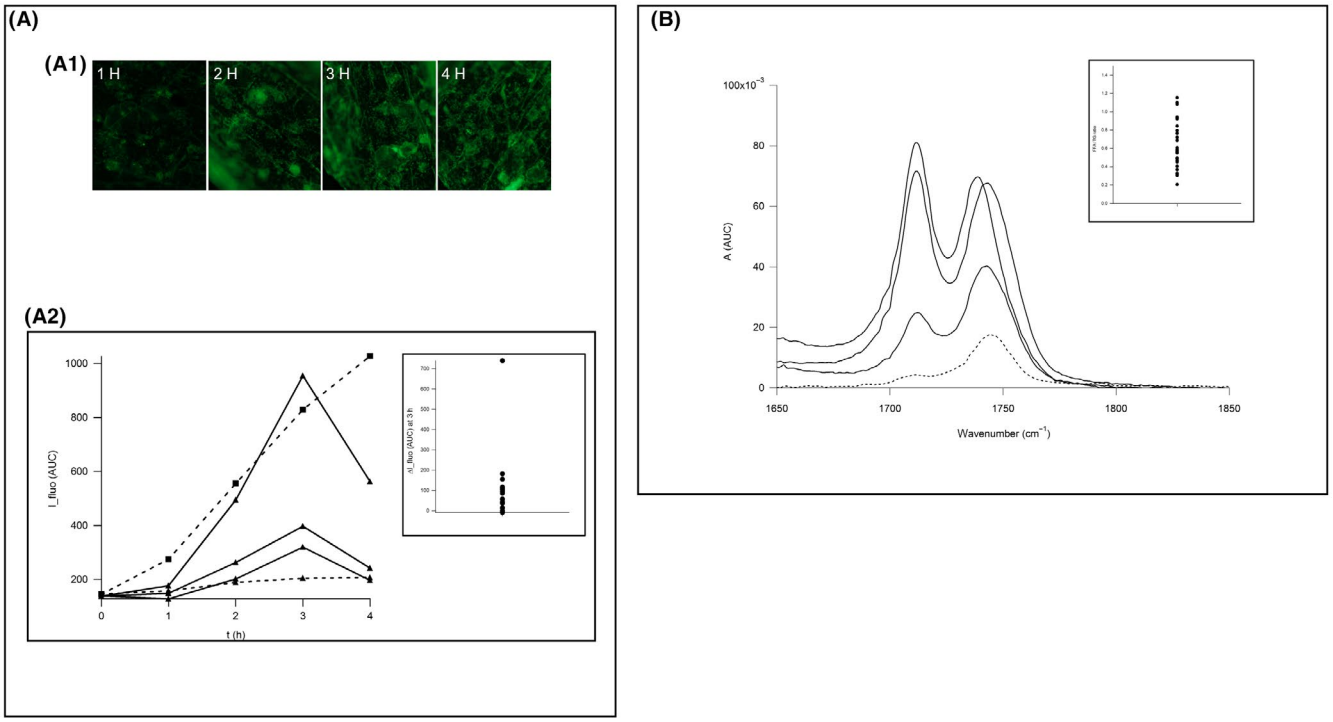

FIGURE 4 Endogenous lipase activity. A, Analysis of *Propionibacterium Acnes* endogenous lipase activity directly measured on CSSS samples using the EnzCheck® substrate. A1, Image at different times showing the fluorescence increase. A2, Fluorescence quantification during time (dotted line with squares: lipase of porcine pancreas as positive control; dotted line with triangles: blank; full line with triangles: microcomedones samples). In small: variation in fluorescence intensity at 3H for all samples. B, Determination by FTIR of free fatty acids (FFA)/ triglycerides (TG) ratio from microcomedones. FTIR spectra of microcomedones samples (full line) compared to a spectra of normal skin sebum (dotted line). In small: FFA/TG ratio for all samples

Figure 3A1). Interestingly, we observed a high correlation (linear correlation coefficient r = .85) between fluorescence intensity (area under the curve computed between 560-665 nm) and the porphyrin amount determined by HPTLC analysis Figure 3A3). This observation confirms that the red fluorescence of comedones really is due to porphyrins.

Secondly, CSSS samples were directly imaged with multiphoton microscopy without staining. The 3D structure of CSSS samples, and particularly of microcomedones, was well defined in autofluorescence mode Figure 3B. A complementary measurement was performed with a spectral detector. The 3D image was then divided into several zones according to different fluorescence signals. Interestingly, microcomedones (inner zone) presented a fluorescence profile closely corresponding to the reference spectrum of porphyrins, with an emission peak around 620 nm (pink curve, Figure 3B3). This signal was very different from that of the other epidermal tissue structures such as corneocytes (blue and yellow curves, Figure 3B3).

Still using porphyrin red autofluorescence properties, skin surface samples obtained by CSSS were then analysed with epifluorescent microscopy. We quantified microcomedone density on mosaic image reconstruction Figure 3C.

All these results showed that intrinsic porphyrin fluorescence can be easily identified in CSSS samples using different methods. This approach also provided a variety of new information: microcomedone density and area, as well as qualitative and quantitative assessment of porphyrins.

3.3 | Endogenous lipase activity

Two complementary approaches were used to evaluate epidermal lipase activity following CSSS. Firstly, endogenous lipase activity was measured directly on cyanoacrylate punches using the EnzChek® lipase substrate. This non-fluorescent substrate was known to produce a green-fluorescent product in the presence of activated lipase. Interestingly, emission of fluorescence was rapidly detected on CSSS with a fluorescence intensity peak between 2 and 3 hours following incubation Figure 4A. These data clearly indicated the presence of biological active lipases in the CSSS samples.

The second approach, using Fourier Transform Infra-Red, was also based on the detection of the enzymatic activity of lipases, which break down triglycerides (TG) into free fatty acids (FFA). Figure 4B depicted a specific IR spectrum of microcomedones extracted from a CSSS sample obtained from acne-prone skin compared to a spectra of normal skin sebum. We identified the specific absorbance peaks of FFA (1710 cm^{-1}) and TG (1740 cm^{-1}). The mean microcomedone FFA/TG ratio of acne-prone subjects was 0.64 ± 0.26. This observation is also supporting the hypothesis of lipolysis due to *P acnes*

colonization. All these data demonstrate the possibly of precisely quantifying endogenous lipase activity from CSSS samples.

4 | DISCUSSION/CONCLUSION

In this study, we provided a complete and precise investigation of microcomedone structure at different magnifications. The MP approach, which was used without any special sample preparation, enabled us to obtain both morphological and constitutive information. Spectral MP imaging was used to directly measure red fluorescence in the microcomedone. The microcomedone material that obstructs the pilosebaceous units was described using 3D MP and SEM views. The imaging analysis showed that microcomedones' structure resembles a pouch, whose interior is mostly composed of lipids with clusters of bacteria and whose outer shell is made up of corneocyte layers. The high bacteria colonization was clearly observed in microcomedones using TEM.

These observations line up with past findings that pilosebaceous unit obstruction and increasing *P acnes* proliferation in microcomedones are likely one of the major factors in the onset of inflammatory acne lesions. Lavker pioneered this approach in 1981 when he used electronic microscopy to point to the relationship between bacteria colonization and follicular keratinization.[22] Moreover, there is probably a size continuity, from very little material in the follicular canal follicular casts (Thielitz et al proposed a size limit of 0.05 mm^2[23]), to structured material that begins to close the canal (microcomedone), and finally to larger comedones that completely obstruct the canal and which are visible by naked eyes.

The spatial organization of *P acnes* colonization in the pilosebaceous unit has been studied by Jahns et al, who immuno-labelled *P acnes* in skin biopsies.[24] They underlined that *P acnes* proliferation in the follicle likely causes the formation of a bacterial biofilm after which, by a quorum-sensing mechanism, bacteria become even more virulent. Optical microscopy studies can be enlarged, however, by the addition of higher resolution images. Our SEM observations confirm that bacteria are present at high density and that colonization is present in the entire volume of the microcomedone. Since it has been established via several techniques that *P acnes* is the main type of bacteria present in microcomedones, we found that it was not necessary to nanogold label the SEM imaging. Moreover, the observed morphology is similar to the morphology of *P acnes* subtype *Propionibacterium acnes subsp nov.* described by Dekio et al.[25]

In the present study, we also showed that red autofluorescence intensity in microcomedones was directly correlated with their porphyrin content. Cornelius et al had already showed in 1967 that this red fluorescence was coming from porphyrins produced by bacteria.[19] In addition, Xu et al confirmed that pure sebum has no red autofluorescence (Xu 2018). The different types of porphyrins produced by *P acnes* were described by Romiti using HPLC.[26] Borelli later showed, in a *vitro* experiment, that porphyrin content was well correlated with *P acnes* quantity.[17] Our observations relative to the porphyrin presence in microcomedones line up with a highly active metabolism of *P acnes*.

Strauss had already proved in 1959 the presence of lipase activity in comedones.[27] Since then, several studies have analysed how the comedone lipid composition is affected by the lipase activity. In the present study, we analysed lipase activity through two practical approaches. First, we followed the breakdown of a fluorescent lipase substrate over time. We observed that lipase activity was clearly present in the extracted microcomedones. Secondly, the free fatty acid/ triglyceride ratio of extracted microcomedones was measured using FTIR. The increasing fatty acid presence, such as palmitic acid, is known to be a triggering signal of the inflammasome response, which plays an important role in the acne pathogenesis.[28,29] Moreover, different level in virulence factors production, such as triacylglycerol lipase, has been identified depending on the strains.[30] And Coenye & al showed that virulence factors, including lipase, are strongly produced in biofilm enhancing the proportion of mono-insaturated fatty acid such as free palmitate which functions as a danger signal stimulating inflammasome via IL1-beta release.[29,31]

In future studies, it will be interesting to follow acne severity over time using these approaches, which combine imaging of bacterial colonization and measurement of bacterial metabolism.

ACKNOWLEDGEMENTS

Electron microscopy studies were performed at the Bordeaux Imaging Center, a Core facility member of the national infrastructure "France BioImaging" (ANR-10-INBS-04 FranceBioImaging).

CONFLICTS OF INTEREST

The authors have no conflict of interest to declare.

AUTHORS' CONTRIBUTION

G. Josse designed the research. C. Mias, J. Le Digabel, J. Filiol, C. Ipinazar, A. Villaret, C. Gomiero, M. Bevilacqua, E. Gontier performed the experiments. T. Nocera, MD, examined the subjects. G. Josse, C. Mias, E. Gontier analysed the data. JH Saurat reviewed the study. G. Josse, C. Mias, D. Redoules wrote the paper. All the authors revised the manuscript.

ORCID

Gwendal Josse https://orcid.org/0000-0003-3375-5226
Céline Mias https://orcid.org/0000-0001-8055-8255

REFERENCES

[1] D. Suh, H. Kwon, *Br. J. Dermatology* **2014**, *172*; 13.
[2] W. J. Cunliffe, D. B. Holland, S. M. Clark, G. I. Stables, *Br. J. Dermatol.* **2000**, *142*, 1084.
[3] S. Moradi Tuchayi, E. Makrantonaki, R. Ganceviciene, C. Dessinioti, S. R. Feldman, C. C. Zouboulis, *Nat. Rev. Dis. Primers*. **2015**, *1*, 15029.
[4] H. Omer, A. McDowell, O. A. Alexeyev, *Clin. Dermatol.* **2017**, *35*, 118.
[5] B. Dréno, S. Pécastaings, S. Corvec, S. Veraldi, A. Khammari, C. Roques, *J. Eur. Acad. Dermatol. Venereol.* **2018**, *32*, 5.

[6] O. A. Alexeyev, B. Lundskog, R. Ganceviciene, R. H. Palmer, A. McDowell, S. Patrick, C. Zouboulis, I. Golovleva, *J. Dermatol. Sci.* **2012**, *67*, 63.
[7] C. C. Zouboulis, *J. Invest. Dermatol.* **2009**, *129*, 2093.
[8] Y. C. Huang, C. H. Yang, T. T. Li, C. C. Zouboulis, H. C. Hsu, *Life Sci.* **2015**, *139*, 123.
[9] G. Plewig, J. E. Fulton, A. M. Kligman, *Arch. Dermatol. Forsch.* **1971**, *242*, 12.
[10] W. J. Cunliffe, D. B. Holland, A. Jeremy, *Clin. Dermatol.* **2004**, *22*, 367.
[11] A. Thielitz, F. Sidou, H. Gollnick, *J. Eur. Acad. Dermatol. Venereol.* **2007**, *21*, 747.
[12] G. Fabbrocini, S. Cacciapuoti, V. De Vita, N. Fardella, F. Pastore, G. Monfrecola, *Dermatology* **2009**, *219*, 322.
[13] J. H. Saurat, *Dermatology* **2015**, *231*, 105.
[14] Z. D. Draelos, J. C. DiNardo, *J. Am. Acad. Dermatol.* **2006**, *54*, 507.
[15] S. V. Patwardhan, C. Richter, A. Vogt, U. Blume-Peytavi, D. Canfield, J. Kottner, *Arch. Dermatol. Res.* **2017**, *309*, 159.
[16] C. Richter, C. Trojahn, G. Dobos, U. Blume-Peytavi, J. Kottner, *Skin Res. Technol.* **2016**, *22*, 451.
[17] C. Borelli, K. Merk, M. Schaller, K. Jacob, M. Vogeser, G. Weindl, U. Berger, G. Plewig, *Acta. Derm. Venereol.* **2006**, *86*, 316.
[18] H. Dobrev, *Photodermatol. Photoimmunol. Photomed.* **2010**, *26*, 285.
[19] C. E. Cornelius, G. D. Ludwig, *J. Invest. Dermatol.* **1967**, *49*, 368.
[20] D. T. Xu, J. N. Yan, W. Liu, X. X. Hou, Y. Zheng, W. W. Jiang, Q. Ju, C. C. Zouboulis, X. L. Wang, *Dermatology* **2018**, *234*, 43.
[21] T. Johnson, D. Kang, E. Barnard, H. Li, *mSphere* **2016**, *1*, e00023-15.
[22] R. M. Lavker, J. J. Leyden, K. J. McGinley, *J. Invest. Dermatol.* **1981**, *77*, 325.
[23] A. Thielitz, M. Helmdach, E. M. Röpke, H. Gollnick, *Br. J. Dermatol.* **2001**, *145*, 19.
[24] A. C. Jahns, H. Eilers, R. Ganceviciene, O. A. Alexeyev, *Br. J. Dermatol.* **2015**, *172*, 981.
[25] I. Dekio, R. Culak, R. Misra, T. Gaulton, M. Fang, M. Sakamoto, M. Ohkuma, K. Oshima, M. Hattori, H. P. Klenk, D. Rajendram, S. E. Gharbia, H. N. Shah, *Int. J. Syst. Evol. Microbiol.* **2015**, *65*, 4776.
[26] R. Romiti, M. Schaller, K. Jacob, G. Plewig, *Arch. Dermatol. Res.* **2000**, *292*, 320.
[27] J. S. Strauss, H. Mescon, *J. Invest. Dermatol.* **1959**, *33*, 191.
[28] R. G. Snodgrass, S. Huang, I. W. Choi, J. C. Rutledge, D. H. Hwang, *J. Immunol.* **2013**, *191*, 4337.
[29] E. Contassot, L. E. French, *J. Invest. Dermatol.* **2014**, *134*, 310.
[30] C. Holland, T. N. Mak, U. Zimny-Arndt, M. Schmid, T. F. Meyer, P. R. Jungblut, H. Brüggemann, *BMC Microbiol.* **2010**, *10*, 230.
[31] T. Coenye, E. Peeters, H. J. Nelis, *Res. Microbiol.* **2007**, *158*, 386.

How to cite this article: Josse G, Mias C, Le Digabel J, et al. High bacterial colonization and lipase activity in microcomedones. *Exp Dermatol*. 2020;29:168–176. https://doi.org/10.1111/exd.14069